Ocean Engineering 266 (2022) 112780

Contents lists available at ScienceDirect

Ocean Engineering

journal homepage: www.elsevier.com/locate/oceaneng

Virtual-reality-based online simulator design with a virtual simulation system for the docking of unmanned underwater vehicle

Hongjuan Li [a,b], Fanghao Huang [a,c,d,*], Zheng Chen [a,c,d]

[a] State Key Laboratory of Fluid Power and Mechatronic Systems, Zhejiang University, 310027, Hangzhou, People's Republic of China
[b] School of Mechanical Engineering, Zhejiang University, 310027, Hangzhou, People's Republic of China
[c] Donghai Laboratory, Zhoushan, 316021, People's Republic of China
[d] Ocean College, Zhejiang University, Zhoushan, 316021, People's Republic of China

ARTICLE INFO

Keywords:
Virtual reality
Underwater docking navigation
Online simulator
Fuzzy PID controller
Unmanned underwater vehicle

ABSTRACT

The simulation of the docking process is an important solution for the control and navigation design of Unmanned Underwater Vehicle (UUV), which can be used to evaluate the reliability of the algorithm in an economic way. However, most of the existing simulations are offline, which cannot interact with the real sensors mounted on the UUV, and cannot visually simulate and display the immersive motion of the UUV in the underwater environment. Therefore, to address the aforementioned problem, an online simulator is designed in this paper, which provides a virtual simulation system for the docking task simulation of the UUV. Two modes are designed with one to provide the virtual simulation with simulated UUV model and sensor, while another to provide the real platform simulation with intuitive visualization of the real tasks achieved by the recorded data. The host and lower computers are designed to communicate and exchange the data. Namely, the lower computer can calculate the mathematical model, and simulate or interact with the real sensor during the docking process; The host computer can obtain the simulated or recorded data from the lower computer, and implement the navigation and control of the UUV, which can be finally displayed in the accurately created virtual docking scene. The fuzzy PID controller and four different navigation modes are designed to implement the experiment with the specific motion verification and underwater docking for the UUV, and the results verify the effectiveness of the online simulator for the underwater tasks simulation with lower cost.

1. Introduction

With the development of science and technology (Wang et al., 2021a; Chen et al., 2020b,a; Sun et al., 2016; Yuan et al., 2019; Huang et al., 2022a), Unmanned Underwater Vehicle (UUV) is playing an important role in the underwater monitoring due to its advantages of wide operation range, good mobility and high intelligence. However, due to the limit of energy carried by the UUV, there are restrictions on its working time and sailing distance. Therefore, the UUV needs to regularly implement the docking tasks back to the docking station for the energy replenishment and the data communication.

Since the UUV has no cable and the docking station has no fixed base, and the underwater currents will lead to the movement of the docking station during the docking process, it is hard to accurately obtain the coordinate of the docking point (Mu et al., 2021; Wang et al., 2021b). Therefore, it is urgent to have a navigation and control system for the UUV to accomplish the docking process with higher accuracy (Sahoo et al., 2019; Melo and Matos, 2017). To verify the effectiveness of the navigation and control system, and make the docking successful, multiple underwater experiments with a highly skilled team and the complicated and high-cost devices are needed, but these repetitive and frequent underwater tasks are difficult to be implemented due to the unpredictable and complicated underwater environments.

The use of simulation provides a new solution to verify the navigation and control system of UUV with a lower cost. The traditional way of simulation is to use the offline simulators (e.g., MATLAB/Simulink) to evaluate the feasibility of the algorithm in the docking tasks, which has the advantages of high programming efficiency, efficient and convenient matrix and array operation (Zhang et al., 2018; Qi et al., 2020; Makavita et al., 2019). However, the implement of the algorithm highly depends on the information directly obtained from the actual docking process, but the offline simulator cannot interact with the real sensors efficiently due to the technical limitations, which results in the

* Corresponding author at: State Key Laboratory of Fluid Power and Mechatronic Systems, Zhejiang University, 310027, Hangzhou, People's Republic of China.
E-mail addresses: lihongjuan@zju.edu.cn (H. Li), huangfanghao@zju.edu.cn (F. Huang), zheng_chen@zju.edu.cn (Z. Chen).

https://doi.org/10.1016/j.oceaneng.2022.112780
Received 21 July 2021; Received in revised form 27 February 2022; Accepted 1 October 2022
Available online 8 November 2022

low efficiency of cyclic operation. Therefore, when using the offline simulators to simulate the complicated docking process, researchers will encounter various problems.

Recently, with the development of computer science, the technology of virtual reality is becoming increasedly mature. As an application of virtual reality, the online simulator with virtual simulation system can combine the virtual scene with real information, and has been widely used in the robot operation training, task planning and other related tasks (Huang et al., 2022b). Namely, Q. Wang et al. design a virtual reality based robot-assisted welding system by obtaining the operator's hand information, which can be used to direct the remote welding tasks of robots (Wang et al., 2020). C. Faure et al. introduce a virtual simulation system, which realizes the control training task of Cable-Driven Robot by capturing the information of the human motion and performing the force perception and visual feedback (Faure et al., 2020). D. T. Kluger et al. construct a virtual reality environment, which assists the study of control algorithms for the prosthetic limbs through the physical model embedded in the virtual prosthetic hand (Kluger et al., 2019). J. I. Lipton et al. design a low-cost telerobotic system, which reconstructs the environment via the video signal and other sensors in the factory, so as to complete the remote equipment acquisition, assembly and manufacturing tasks more efficiently and accurately (Lipton et al., 2018). M. Peral-Boiza et al. develop a virtual training platform for a minimally invasive surgical robot, which can be used to train the doctors in the operation of flexible ureterorenoscope (Peral-Boiza et al., 2019).

Therefore, most of the existing virtual simulation systems mentioned above are used in the terrestrial environment. Since the use of simulation provides a new solution of underwater tasks with a lower cost, some researchers preliminarily investigate the virtual simulation system for the underwater robots (e.g., AUV, ROV, UUV). Namely, Monferrer et al. propose a series of guidelines in terms of the operation interface, and the simulation technology is based on an enhanced human machine interface for the underwater operations (Monferrer and Bonyuet, 2002; Bruno et al., 2019). Marcos et al. develop a virtual simulation system for the ROV, which can simulate the complicated underwater operations (e.g., salvage the black box) with the virtual environment image captured by the ROV (de la Cruz et al., 2020). Ahmad et al. develop a simulator enhanced by the multipurpose fuzzy region, which enables the operator to carry out the simulation tests of various algorithms for the underwater robots without the understanding of the graphics programming (Bukhari and Kim, 2013). Y. Nie et al. design a simulator to simulate the effect of random currents on the underwater glider by importing the real underwater data (Nie et al., 2020).

However, most of the existing underwater virtual simulation systems have the drawbacks of low image frame rate and lack of interaction with the real sensors mounted on the underwater robots, which result in the poor ability to simulate the complicated tasks with multi-sensor sensing and collaboration. Besides, few researches are carried out for the specific underwater tasks (e.g., docking, navigation, motion control, etc.). Therefore, to address the aforementioned problems, an online simulator with virtual simulation system is designed in this paper for the specific docking task of the UUV. This online simulator provides a virtual platform of the underwater scene, and a convenient and effective experimental tool for the research of navigation and control problems for the UUV with a lower cost. The main contributions are as follows:

(1) The online simulator can real-time simulate or interact with multiple sensors mounted on the real UUV in the docking process, which can guarantee the authenticity of the virtual underwater tasks;

(2) The integrated navigation modes are designed combining the four docking modes, which includes the hybrid navigation of the inertial navigation system and doppler speedometer, the acoustic navigation system, the image navigation system and the light navigation system;

(3) The mathematical model and the fuzzy PID controller are designed to implement the motion control of UUV in the virtual simulation system;

(4) The navigation and control algorithms (e.g., integrated navigation modes and fuzzy PID controller) run in the host computer, while the mathematical model combined with the sensor data runs in the lower computer. Through the communication of host and lower computers, the navigation and control problems can be verified, and the immersive motion of the UUV can be displayed in the virtual simulation system with the real-time recorded data, which provides an open interface that allows the researchers to test and improve their algorithms by the simulation of underwater docking process before the real underwater test.

The rest of this paper is organized as follows. Section 2 introduces the overall framework of the virtual simulation system, and Section 3 presents the design of each unit for the virtual simulation system. Section 4 selects the motion verification and underwater docking to implement the application demonstration of the underwater tasks for the UUV. Section 5 presents the conclusion.

2. Overall framework of virtual simulation system

Using the virtual reality technology, an online simulator with virtual simulation system is designed for the docking task of UUV, which can be used to simulate the docking process, with regard to the real underwater environment and the data communication both in the virtual and real platform simulation. The virtual simulation system mainly consists of the virtual docking scene, data monitoring unit, docking navigation unit, motion and control unit and environmental perception and localization unit, which can be used to verify the stability and reliability of the UUV in the docking process.

However, considering the complexity and the expensive cost of the underwater tests, it is usually difficult to frequently implement the docking tasks of the UUV in the real underwater environment. Thus, the proposed virtual simulation system has the following two modes:

•**Mode 1**: The virtual simulation of underwater docking tasks with the simulated UUV model and sensor. This mode allows the researchers to test and improve their algorithms by the simulation of underwater docking process before the real underwater test, which can be achieved by the help of data communication among these units of the virtual simulation system under the simulated UUV model and sensor.

•**Mode 2**: The real platform simulation of underwater docking task with the recorded in-situ data obtained from the real UUV. Considering that the actual docking process cannot be observed in real time, this mode allows the virtual simulation system to accurately imitate the actual docking process with the recorded in-situ data, which can be used to observe the technical problem and optimize them before the next test.

Based on these two modes, the flow chart of the virtual simulation system is shown in Fig. 1.

When performing the virtual simulation, as shown by the blue line in Fig. 1, the host computer runs in the Matlab/Simulink environment, the lower computer runs in the Unity simulation software, and the communication between the host and the lower computers are achieved by the TCP/IP communication. Based on the location of the UUV and the docking point, the control unit calculates the control inputs (e.g., propeller velocity, rudder angle of UUV), which are obtained from the Matlab/Simulink and transmitted to the motion unit, thus finishing the motion simulation of the UUV with regard to its kinematics, dynamics and related control algorithms. In the meantime, based on the distance between the UUV and the docking point, which is obtained from the environmental perception and localization unit, different docking modes are selected with regard to the navigation strategy in the docking navigation unit. Therefore, by constantly updating the data (obtained from simulated sensor) to the environmental perception and localization unit, the docking navigation

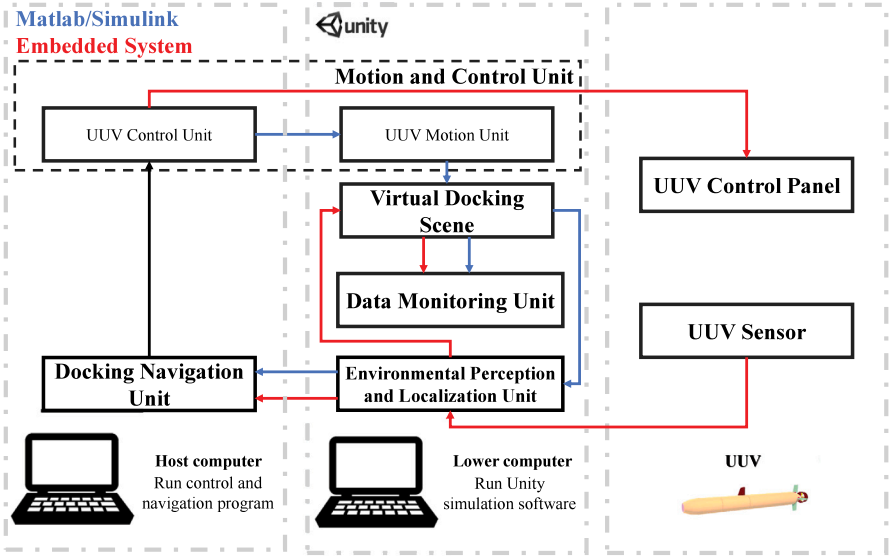

Fig. 1. The flow chart of virtual simulation system. (For interpretation of the references to color in this figure legend, the reader is referred to the web version of this article.)

unit can select diffident navigation modes, and the motion and control unit can simulate the motion of UUV to the docking point. The entire process is displayed on the virtual docking scene. The data monitoring unit can display the roll, pitch and heading angles, velocity, latitude and longitude in the location of the UUV, and draw the trajectory in real time.

When performing the real platform simulation, as shown by the red line in Fig. 1, the host computer runs in the embedded system mounted on the real UUV, which is used to drive the motion of the UUV and record the sensor data, and the lower computer still runs in the Unity simulation software. After the actual docking process, the recorded sensor data can be transmitted from the host computer to the lower computer under the serial communication. Based on the location of the UUV and the docking point obtained from the real sensors, the control unit calculates the control inputs, which are obtained from the embedded system and transmitted to the real UUV control panel to drive its motion in the real underwater environment. The related data obtained from the sensor mounted on the UUV are recorded and transmitted to the lower computer after the actual docking process, which are used to reconstruct the motion and docking process of the UUV in the virtual docking scene, while the data are displayed real-time in the data monitoring unit.

3. Unit design for virtual simulation system

3.1. Virtual docking scene design

Based on the real underwater environment, a virtual docking scene of UUV is established in the system, which mainly includes the docking task scene and underwater environment. Among them, the docking task scene mainly includes the 3D modeling of the UUV and the docking station.

3.1.1. Docking task scene modeling

Based on the real UUV structure shown in Fig. 2(a), a proportional 3D model of UUV is built by the SolidWorks software, as shown in Fig. 2(b). A tail propeller is used as the power system, where a cross rudder is used to control the direction of the motion for the UUV. With regard to its motion, two coordinate systems are defined, which include the ground coordinate system and the carrier coordinate system. Supposing that the positive direction of X axis for the UUV model is the positive direction of the motion, the UUV model is rotated

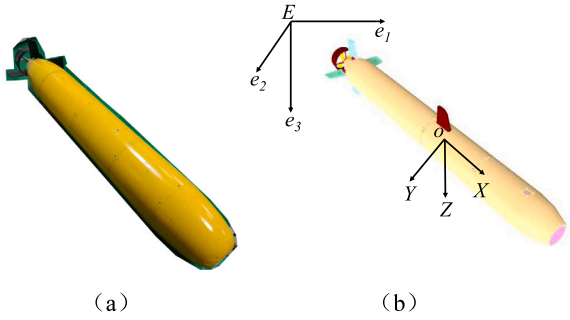

Fig. 2. The modeling of UUV. (a) the real UUV structure; (b) the proportional 3D model of the UUV.

in the Unity simulation software to guarantee that the heading direction of the UUV is always the positive direction of X axis.

Moreover, to ensure that the 3D model of UUV can physically simulate the motion of the real UUV during the docking process, some facilities (e.g., inertial navigation system, doppler velocimeter, CCD camera, etc.) carried on the UUV are also added in this 3D model, and the detailed physical principle is described in Section 3.3.

Similarly, a proportional 3D model of docking station is built by SolidWorks software, as shown in Fig. 3. The light of base station is simulated through the visual effect module in the Unity simulation software as the green light, which can also been seen in Fig. 3.

3.1.2. Underwater environment modeling

With regard to the real video signal obtained from the previous underwater test, the underwater environment is modeled in the virtual docking scene. Based on the random function in *C#* language, a random underwater current is established, whose flow velocity and direction change with time. The velocity range is 0–0.25 m/s, and the direction range is 0–360°.

To accurately create the underwater environment, three parts are designed including the sea level, the underwater area and the seabed topography. In the sea level, to well simulate the influence of the wave and current, which is generated by the wind, the Crest plug-in in the Unity simulation software, which is based on the Gerstner wave function, is used to imitate the geometric shape of the wave and

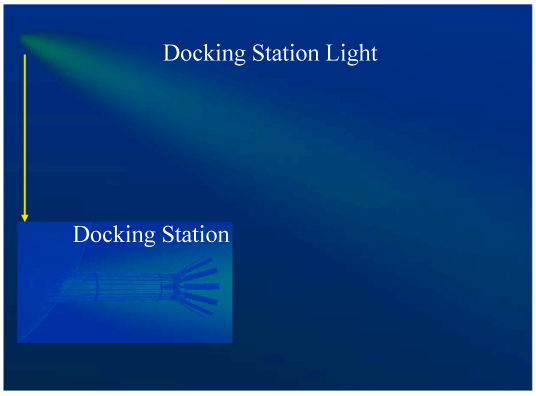

Fig. 3. The 3D model of docking station and its light.

current. The detailed Gerstner wave function is defined as follows:

$$x_g = x_{g0} - \sum_{i=1}^{n}\sum_{j=1}^{m} \cos\theta_j a_{ij} \sin\left(k_i\left(x_{g0}\cos\theta_j + z_{g0}\sin\theta_j\right) - \omega_i t + \varphi_i\right) \quad (1)$$

$$y_g = y_{g0} + \sum_{i=1}^{n}\sum_{j=1}^{m} a_{ij} \cos\left(k_i\left(x_{g0}\cos\theta_j + z_{g0}\sin\theta_j\right) - \omega_i t + \varphi_i\right) \quad (2)$$

$$z_g = z_{g0} - \sum_{i=1}^{n}\sum_{j=1}^{m} \sin\theta_j a_{ij} \sin\left(k_i\left(x_{g0}\cos\theta_j + z_{g0}\sin\theta_j\right) - \omega_i t + \varphi_i\right) \quad (3)$$

where (x_{g0}, y_{g0}, z_{g0}) is the initial position of a wave or current point in the current coordinate system, (x_g, y_g, z_g) is the updated position of a wave or current point after the calculation by the Gerstner wave function, $i = 1{-}n$, $j = 1{-}m$, n is the partition number of the frequencies, m is the partition number of the directions, that is, the total number of simulated waves or currents is $n \times m$, a_{ij} is the amplitude of the wave or current, k_i is the number of the wave or current, ω_i is the angular frequency, φ_i is the initial phase angle, θ_j is the angle along the X axis on the XZ plane. Based on the kinematics and dynamics of the UUV in Section 3.2.1 and the physics engine in the Unity simulation software, the simulation of the waves or currents' motion on the sea level is achieved, where the UUV can moves along the waves or currents, as shown in Fig. 4(b)–(c). Particularly, the simulated UUV on the sea level under the influence of the waves and currents is accurately created when compared with Fig. 4(a), which shows the real test condition of the UUV on the sea level.

In the underwater area, the color and transparency are modified by the atomization plug-in in the Unity simulation software, which can simulate that the deeper the underwater area, the darker the visual effect, as shown in Fig. 4(d)–(e). In the seabed topography, the raw data file in a certain terrain near Zhoushan, China is built and merged by the Height Mapper plug-in in the Unity simulation software, as shown in Fig. 4(f).

3.2. Motion and control unit design

The motion and control unit mainly includes the mathematical modeling and motion control of UUV, who has the tail thruster and cross rudder.

3.2.1. Motion unit design

The kinematics and dynamics of the UUV can be written as:

$$\dot{\eta} = J(\eta)V \quad (4)$$

$$M\dot{V} + C(V)V + D(V)V + g(\eta) = \tau \quad (5)$$

where $\eta = [x, y, z, \varphi, \theta, \psi]^T$ are the position, roll, pitch and heading angle of UUV, $V = [u, v, w, p, q, r]^T$ are the velocity and angular velocity of the UUV in X, Y and Z axis respectively, M is the mass matrix, $C(V)$ is the coriolis and centripetal matrix, $D(V)$ is the hydrodynamics matrix, $g(\eta)$ is the gravity and buoyancy matrix, τ is the control input matrix, $J(\eta)$ can be defined as:

$$J(\eta) = \begin{bmatrix} R(\varphi,\theta,\psi) & 0_{3\times3} \\ 0_{3\times3} & T(\varphi,\theta) \end{bmatrix} \quad (6)$$

$$R(\varphi,\theta,\psi) = \begin{bmatrix} c\theta c\psi & s\varphi s\theta c\psi - c\varphi s\psi & c\varphi s\theta c\psi + s\varphi s\psi \\ c\theta s\psi & s\varphi s\theta s\psi + c\varphi c\psi & c\varphi s\theta s\psi - s\varphi c\psi \\ -s\theta & s\varphi c\theta & c\varphi c\theta \end{bmatrix} \quad (7)$$

$$T(\varphi,\theta) = \begin{bmatrix} 1 & s\varphi t\theta & c\varphi t\theta \\ 0 & c\varphi & -s\varphi \\ 0 & s\varphi/c\theta & c\varphi/c\theta \end{bmatrix} \quad (8)$$

Considering the low velocity of UUV in the docking process, the matrix $D(V)$ is ignored, and the gravity and buoyancy are offset as $g(\eta) = 0$. Therefore, the dynamics (5) can be simplified as:

$$M\dot{V} + D(V)V = \tau \quad (9)$$

Particularly, under the influence of the current, the orientation of the current coordinate system is consistent with that of the ground coordinate system, so the projection of the UUV's velocity in the carrier coordinate system, which is relative to the current coordinate system, is defined as $V_w = [u_w, v_w, w_w, p_w, q_w, r_w]^T$, and the velocity of the current in the ground coordinate system is defined as $V_{WE} = [u_{WE}, v_{WE}, w_{WE}, 0, 0, 0]^T$, which can be derived from (1)–(3). Therefore, in the current coordinate system, the UUV can be regarded as moving in the static environment, and the kinematics and dynamics of the UUV are the functions of V_w, which can be written as follows:

$$\dot{\eta} = J(\eta)V_w + V_{WE} \quad (10)$$

$$M\dot{V}_w + D(V_w)V_w = \tau \quad (11)$$

In (8), the matrices M and $D(V_w)$ are defined as:

$$M = \begin{bmatrix} m - X_{\dot{u}_w} & 0 & 0 & 0 & 0 & 0 \\ 0 & m - Y_{\dot{v}_w} & 0 & 0 & 0 & -Y_{\dot{r}_w} \\ 0 & 0 & m - Z_{\dot{w}_w} & 0 & -Z_{\dot{q}_w} & 0 \\ 0 & 0 & 0 & K_{\dot{p}_w} & 0 & 0 \\ 0 & 0 & -M_{\dot{w}_w} & 0 & I_y - M_{\dot{q}_w} & 0 \\ 0 & -N_{\dot{v}_w} & 0 & 0 & 0 & I_z - N_{\dot{r}_w} \end{bmatrix} \quad (12)$$

$$D(V_w) = \begin{bmatrix} X_{u_w}u_w + X_{u_w} & mr_w & -mq_w & 0 & 0 & 0 \\ 0 & Y_{v_w} & 0 & 0 & 0 & Y_{r_w} - mu_w \\ 0 & 0 & Z_{w_w} & 0 & Z_{q_w} + mu_w & 0 \\ 0 & 0 & 0 & K_{p_w} & 0 & 0 \\ 0 & 0 & M_{w_w} & 0 & M_{q_w} & 0 \\ 0 & N_{v_w} & 0 & 0 & 0 & N_{r_w} \end{bmatrix} \quad (13)$$

where m is the mass of UUV, I_y and I_z are the momentum of inertia in Y and Z axis, other parameters are the hydrodynamics parameters. Note that the main work of this paper is to create an online simulator to provide an open interface that allows the researchers to test and improve their algorithms, many works related to the modeling of these hydrodynamics parameters can refer to Sarhadi et al. (2016), Miao et al. (2017) and be achieved by programming in this simulator.

3.2.2. Control unit design

The control unit is designed to control the rudder angle and propeller velocity based on the data obtained from the UUV sensor, which can achieve the motion of the UUV to accomplish the docking task. Note that any algorithm developed by the researchers can be programmed in the Matlab/Simulink environment or embedded system of the proposed online simulator, here we take the fuzzy PID controller for example to illustrate the principle of the control unit (Huang

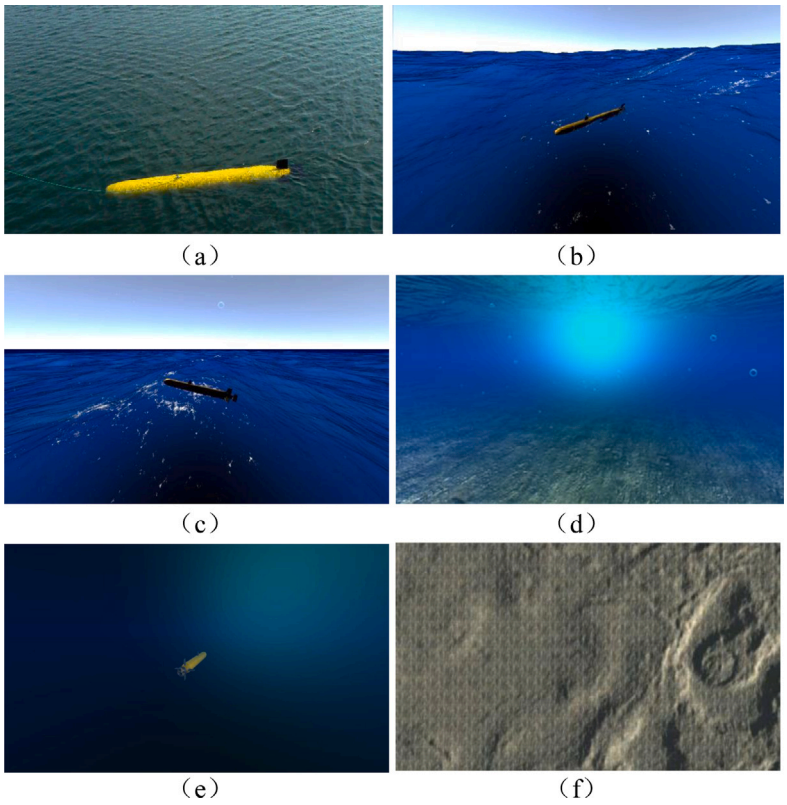

Fig. 4. The underwater environment modeling. (a) the sea level in the real underwater test; (b) the sea level with UUV posture 1 in the virtual docking scene; (c) the sea level with UUV posture 2 in the virtual docking scene; (d) the shallow underwater area in the virtual docking scene; (e) the deep underwater area in the virtual docking scene; (f) the seabed topography in the virtual docking scene.

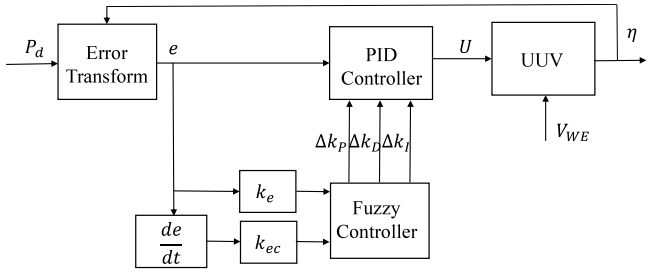

Fig. 5. The flowchart of fuzzy PID controller.

et al., 2018). In detail, the propeller force and rotation of two rudder angles are used as the control variables, by the process of fuzzification and defuzzification, the control of the rudder angle and the propeller velocity of each rudder is finally achieved.

The flowchart of the fuzzy PID controller is shown in Fig. 5. For the simple implementation, define $P_d = [x_a, y_a, z_a]^T$ as the desired docking point, k_e and k_{ec} are the quantization factors related to e and ec, and Δk_P, Δk_I and Δk_D are the rete of change in parameters of PID controller. The influence of the current mainly characterizes as the velocity of the current V_{WE} in Fig. 5. Since the control input τ in Eq. (9) can be calculated with regard to the propeller, horizontal rudder angle and vertical rudder angle (Wang et al., 2010), define the new control input as $U = [n, \delta_s, \delta_t]^T$, where n is the velocity of propeller, δ_s and δ_t are the horizontal and vertical rudder angles respectively.

The error transform for $e = [e_d, e_\theta, e_\psi]^T$ can be defined as:

$$e_d = \sqrt{(x_a - x)^2 + (y_a - y)^2 + (z_a - z)^2} \tag{14}$$

$$e_\theta = \sin\left(\theta - \arctan\left(\frac{z_a - z}{x_a - x}\right)\right) \tag{15}$$

Table 1
The fuzzy rule of Δk_p.

Δk_P		ec						
		NB	NM	NS	ZO	PS	PM	PB
e	NB	PB	PB	PM	PM	PS	ZO	ZO
	NM	PB	PB	PM	PS	PS	ZO	NS
	NS	PM	PM	PM	PS	ZO	NS	NS
	ZO	PM	PM	PM	ZO	NS	NM	NM
	PS	PS	PS	ZO	NS	NS	NM	NM
	PM	PS	ZO	NS	NM	NM	NM	NB
	PB	ZO	ZO	NM	NM	NM	NB	NB

Table 2
The fuzzy rule of Δk_I.

Δk_I		ec						
		NB	NM	NS	ZO	PS	PM	PB
e	NB	NB	NB	NM	NM	PS	ZO	ZO
	NM	NB	NB	NM	NS	NS	ZO	ZO
	NS	NB	NM	NS	NS	ZO	PS	PS
	ZO	NM	NM	NS	ZO	PS	PM	PM
	PS	NM	NS	ZO	PS	PS	PM	PB
	PM	ZO	ZO	PS	PS	PM	PB	PB
	PB	ZO	ZO	PS	PM	PM	PB	PB

$$e_\psi = \sin\left(\psi - \arctan\left(\frac{y_a - y}{x_a - x}\right)\right) \tag{16}$$

Then, the input of fuzzy controller are defined as e and ec, the output are defined as Δk_P, Δk_I and Δk_D, and the range of discourse domain are $[-6, 6]$. If the input range $[i, j]$ is not in $[-6, 6]$, it will be transformed as $\frac{12}{j-i}\left(x + \frac{i+j}{2}\right)$. The membership function of fuzzy controller is shown in Fig. 6, and the fuzzy rules are shown in Tables 1–3, where NB is negative big, NM is negative medium, NS is negative

Table 3
The fuzzy rule of Δk_D.

Δk_D		ec						
		NB	NM	NS	ZO	PS	PM	PB
e	NB	PS	NS	NB	NB	NB	NM	PS
	NM	PS	NS	NB	NM	NM	NS	ZO
	NS	ZO	NS	NM	NM	NS	NS	ZO
	ZO	ZO	NS	NS	NS	NS	NS	ZO
	PS	ZO	ZO	ZO	ZO	ZO	ZO	ZO
	PM	PB	NS	PS	PS	PS	PS	PB
	PB	PB	PM	PM	PM	PS	PS	PB

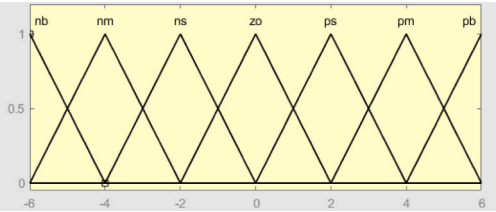

Fig. 6. The membership function of fuzzy PID controller.

small, ZO is zero, PS is positive small, PM is positive medium, PB is positive big.

After the fuzzy control to obtain the Δk_p, Δk_I and Δk_D, the PID controller U can be obtained as:

$$U = K_P \cdot e + K_I \int edt + K_D \cdot \frac{de}{dt} \tag{17}$$

where K_P, K_I and K_D can be updated by Δk_P, Δk_I and Δk_D.

3.3. Environmental perception and localization unit design

The environmental perception and localization unit mainly includes the simulated inertial navigation system, doppler speedometer and CCD camera. This unit can be used to calculate the simulated information posture, velocity and angular velocity of the UUV, as well as the optical signal in the virtual simulation system, or accurately obtain the same data from the real sensor. Therefore, the data simulated or recorded can be transmitted to accomplish the navigation of the UUV to the docking station.

3.3.1. The inertial navigation system

The inertial navigation system uses TCP/IP multicast to send the message, where the sending frequency is 10 Hz, the IP address is 224.0.1.1, and the port number is 8080.

The principle of the inertial navigation system is as follows. Firstly, obtain the velocity and acceleration based on (11). Secondly, by collecting the posture and angular velocity of the UUV in three directions of roll, pitch and bow, it is packaged into a TCP/IP message and sent to the multicast at a fixed frequency. Finally, the relative position of the UUV and the docking point is calculated through the attitude angle and the angular velocity, which can guide the UUV to move to the docking point, thereby realizing the navigation.

3.3.2. The doppler speedometer

The doppler speedometer uses TCP/IP multicast to send the message, where the sending frequency is 10 Hz, the IP address is 224.0.1.1, and the port number is 8081.

The principle of the doppler speedometer is as follows. Based on the real doppler speedometer data, four beams are emitted downward, with regard to the principle of the acoustic reflection, and the beam collision detection method in the Unity simulation software, the echo frequencies of the different beams can be obtained, and are packaged into a TCP/IP message and sent to the multicast at a fixed frequency.

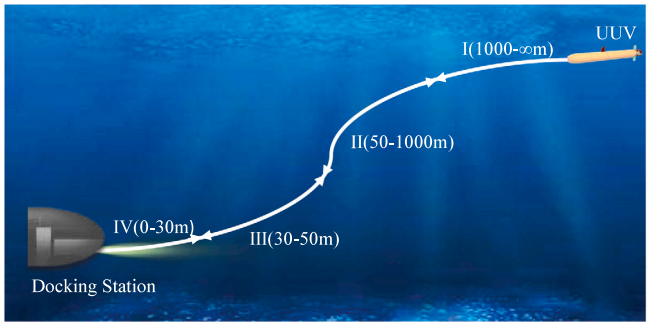

Fig. 7. The four navigation modes in docking navigation unit.

Therefore, with regard to the echo frequencies of different beams, the velocity of the UUV relative to the ground coordinate system can be calculated, thereby assisting the inertial navigation system to complete the navigation.

3.3.3. The CCD camera

The CCD(charge couple device) camera uses TCP/IP multicast to send the message, where the sending frequency is 10 Hz, the IP address is 224.0.1.1, and the port number is 8082.

The principle of the CCD camera is as follows. Based on the camera plug-in in the Unity simulation software, it is placed in front of the UUV to simulate the shooting of underwater environment and used to obtain the image in front of the UUV. The CCD camera takes a screenshot of the acquired image at a frequency of 10 Hz, and packs it into a TCP/IP message and sends it to the multicast at a fixed frequency. By calculating the pixel information, the relative position between the UUV and the docking point can be obtained, thereby assisting the inertial navigation system to complete the navigation.

3.4. The docking navigation unit design

During the docking process between the UUV and the docking station, since the docking station is not fixed, its accurate position cannot be obtained, and there are usually problems such as the shaking due to the underwater current. Therefore, the control of the docking process cannot completely rely on the calculation. In order to guarantee the high accuracy of the docking process, four different navigation modes are designed in the docking navigation unit with regard to the distance between the UUV and the docking station, including: (I) Remote docking guidance, (II) Medium and long distance docking guidance, (III) Medium and short distance docking guidance, (IV) Final docking guidance, which is shown in Fig. 7.

3.4.1. The remote docking guidance

Since the location of the UUV is obtained by the integral calculation of the inertial navigation system, it is prone to accumulate larger errors in the case of long-term navigation, so the correction of its location is needed. Note that the global positioning system (GPS) can only be used on the surface of the water, when the UUV needs to return to the docking station but the distance between the docking station is far away and located outside the acoustic navigation range, the method of surface correction and underwater navigation is adopted. At first, the UUV natantly obtains its location as X_0, Y_0 and Z_0 with the help of the GPS, and (X_0, Y_0, Z_0) is set as the initial position. To note that, since the UUV natantly obtains its location, the initial position $Z_0 = 0$ m. Subsequently, the inertial navigation system is combined with the doppler speedometer to implement the hybrid navigation, and help navigate the UUV move within the acoustic navigation range.

The detailed principle of the inertial navigation system is in the following. Based on the UUV's posture, position, and velocity at the

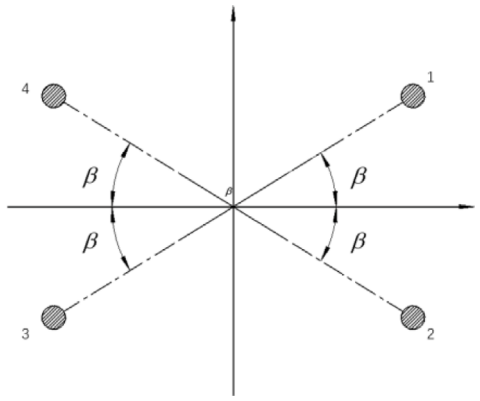

Fig. 8. The horizontal distribution map of four beam doppler system.

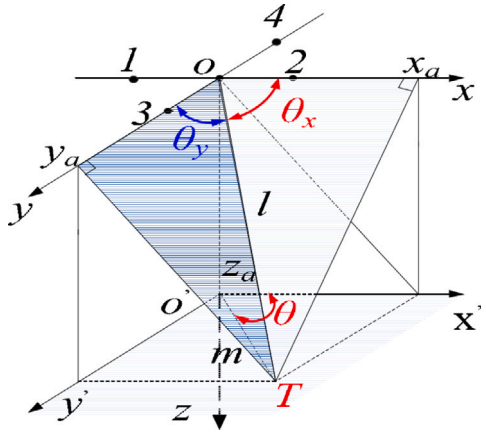

Fig. 9. The principle of USBL navigation system.

last moment, the navigation data of the UUV at each moment can be obtained. Then, based on the ground coordinate system, the basic equation of the inertial navigation system can be obtained as:

$$\dot{V}^n = C^n f - (2\omega_i{}^n + \omega_e{}^n)V^n + g^n \tag{18}$$

where $V = [u, v, w]^T$ is the velocity of UUV in ground coordinate system, $C_n = R(\varphi, \theta, \psi)$, f is the specific force component resolved by inertial device, X, Y and Z are the latitude, longitude and altitude, $\omega_i{}^n = [0, \omega_i \cos X, \omega_i \sin X]^T$ is the angular velocity of earth's rotation, $\omega_e{}^n = [-\frac{u}{R_M+Z}, \frac{v}{R_N+Z}, \frac{w\tan X}{R_N+Z}]^T$, $R_M = \frac{R_e(1-s^2)}{\left(1-s^2\sin^2 X\right)}$, $R_N = \frac{R_e}{\sqrt{(1-s^2)\sin^2 X}}$, R_e is the earth radius, s^2 is the first eccentricity of earth.

Subsequently, the longitude, latitude and altitude of the UUV at the next moment can be obtained as:

$$X = X_0 + \int_0^{T_0} \frac{u}{R_M + Z} dt \tag{19}$$

$$Y = Y_0 + \int_0^{T_0} \frac{v \sec X}{R_N + Z} dt \tag{20}$$

$$Z = Z_0 - \int_0^{T_0} w dt \tag{21}$$

where T_0 is the update cycle.

Therefore, after the transformation, the position of the UUV can be obtained as:

$$x_a = K_m \ln\left(\tan\left(\frac{\pi}{4} + \frac{X}{2}\right)\left(\frac{1 - s^2 \sin X}{1 + e^2 \sin X}\right)^{\frac{s^2}{2}}\right) \tag{22}$$

$$y_a = K_m \left(Y - Y_0\right) \tag{23}$$

$$z_a = Z_0 - Z \tag{24}$$

where $K_m = \frac{R_e}{\left(1-2\sin^2 X\right)} \cos\left(X_0\right)$.

The detailed principle of the doppler speedometer is in the following. Define α as the angle between the beam and the horizontal plane where the UUV is located, β is shown in Fig. 8.

Then, the doppler shifts of the four beams can be obtained as:

$$f_{d1} = 2\left(uA_x + vA_y + wA_z\right)/\lambda \tag{25}$$

$$f_{d2} = 2\left(uB_x + vB_y + wB_z\right)/\lambda \tag{26}$$

$$f_{d3} = 2\left(uC_x + vC_y + wC_z\right)/\lambda \tag{27}$$

$$f_{d4} = 2\left(uD_x + vD_y + wD_z\right)/\lambda \tag{28}$$

where λ is the wavelength, $A_i, B_i, C_i, D_i\ (i = x, y, z)$ are the directional cosines of four beams, and satisfy:

$$A_x = B_x = -C_x = -D_x = \cos\alpha\cos\beta \tag{29}$$

$$A_y = B_y = C_y = D_y = -\sin\alpha \tag{30}$$

$$-A_z = B_z = C_z = -D_z = \cos\alpha\sin\beta \tag{31}$$

Therefore, the velocity of the UUV can be obtained as:

$$u = \frac{\lambda\left(f_{d2} - f_{d3}\right)}{4\cos\alpha\cos\beta} \tag{32}$$

$$v = -\frac{\lambda\left(f_{d1} + f_{d3}\right)}{4\sin\alpha} \tag{33}$$

$$w = \frac{\lambda\left(f_{d2} - f_{d1}\right)}{4\cos\alpha\sin\beta} \tag{34}$$

3.4.2. The medium and long distance docking guidance

Since the data of inertial navigation system is generated through the integration, the position error will accumulate over time, which results in the poor accuracy. Therefore, when approaching the acoustic navigation range (at about 50–1000 m), the ultra short baseline(USBL) navigation system is used, where the underwater acoustic signals are used to determine the distance between the UUV and the docking station. The detailed principle of USBL navigation system is in the following.

The USBL navigation system can calculate the slope distance by measuring the round-trip time of the underwater acoustic signals, which is sent by the transmitter and received by the transponder installed on the UUV. The principle is shown in Fig. 9, where the transmitter is set as the origin coordinate O, towards the seabed is defined as the positive direction of Z axis. The four interrogators are located on the X and Y axis of the coordinate system, and the distance between the coaxial interrogators is d, where the coordinate of each interrogator is $\left(\pm\frac{d}{2}, \pm\frac{d}{2}\right)$. The transponder is set as T, with the coordinate as P_d.

Based on the geometric relationship shown in Fig. 9, the coordinate of the transponder, which is also the position of the UUV, can be obtained as:

$$x_a = \frac{\lambda l \varphi_x}{2\pi d} \tag{35}$$

$$y_a = \frac{\lambda l \varphi_y}{2\pi d} \tag{36}$$

$$z_a = \sqrt{l^2 - {x_a}^2 - {y_a}^2} \tag{37}$$

where l is the slope distance, φ_x and φ_y are the angle between l and X-axis or Y-axis.

3.4.3. The medium and short distance docking guidance

The accuracy of acoustic navigation is inversely proportional to the navigation distance, that means, the closer the distance between the UUV and the docking station, the poorer the accuracy. Therefore, when approaching the medium and short distance (at about 30–50 m),

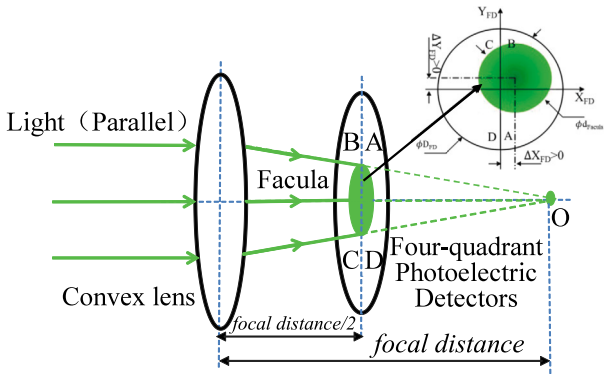

Fig. 10. The principle of light navigation system. (For interpretation of the references to color in this figure legend, the reader is referred to the web version of this article.)

an image navigation system is designed to assist the USBL navigation system and increase the accuracy, which relies on a strong penetrating light as a guide signal. By shooting the light with a CCD camera, the relative position of the UUV and the light can be calculated, which can guide the UUV to approach the docking station. The detailed principle of image navigation system is in the following.

Firstly, the original image is captured by a CCD camera with a capture frequency of 25 Hz. However, due to the scattering of the underwater light, the accurate position of the light in the image coordinate is difficult to be estimated, which should be modified with the image binarization. Therefore, based on the Otsu algorithm, the original image is divided into two parts, which includes the bright group and dark group. Then, the result of the image binarization can be obtained as:

$$p_{ij} = \begin{cases} 1 & p_{ij} > \varsigma \\ 0 & p_{ij} \le \varsigma \end{cases} \tag{38}$$

where ς is the average value of all elements in set Ω, which can be defined as:

$$\Omega = \left\{k^* \mid \delta_B^2\left(k^*\right) = \max_{0\le k\le L-1}\delta_B^2(k), k^* \in [0, L-1]\right\} \tag{39}$$

where L is the number of intensity levels, δ_B^2 is the between-class variance.

Secondly, the noise in the original image after the binarization should be removed. Since the noise area is much smaller than that of the target area in the navigation range, pixels in small connected areas can be removed to eliminate the influence of noise. Select the center of target area as the position of light, the image coordinate can be obtained as:

$$\bar{u}_p = \frac{\Sigma\Sigma_D u_p \times \mu(u_p, v_p)}{\Sigma\Sigma_D \mu(u_p, v_p)} \tag{40}$$

$$\bar{v}_p = \frac{\Sigma\Sigma_D v_p \times \mu(u_p, v_p)}{\Sigma\Sigma_D \mu(u_p, v_p)} \tag{41}$$

where u_p and v_p are the abscissa and ordinate of pixel in the image coordinate after binarization, $\mu(u_p, v_p)$ is the pixel value of image after binarization.

If the range of captured image is $h_x \times h_y$, which means that $\bar{u}_p \in \left[-h_x/2, h_x/2\right]$ and $\bar{v}_p \in \left[-h_y/2, h_y/2\right]$,

The angle between the heading direction of UUV and horizontal/vertical plane of docking station can be obtained as:

$$\beta_s = \arctan\left(2\bar{u}_p/h_x \times \tan\alpha_s\right) \tag{42}$$

$$\theta_s = \arctan\left(2\bar{v}_p/h_y \times \tan\alpha_s\right) \tag{43}$$

where α_s is the viewing angle of the CCD camera.

Finally, by the combination of the image-based relative angles (β_s and θ_s) and the position P_d of the UUV obtained by the USBL navigation system, the navigation in the medium and short distance docking guidance can be achieved.

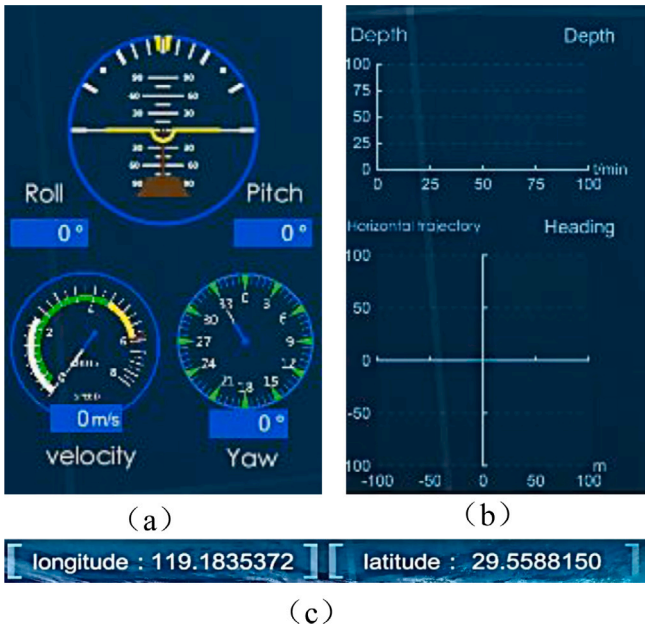

Fig. 11. The data monitoring interface. (a) state monitoring interface; (b) trajectory monitoring interface; (c) longitude and latitude monitoring interface.

3.4.4. The final docking guidance

When approaching the final distance (less than 30 m), the light is bright enough when compared to the medium and short distance. Therefore, based on the USBL navigation system and the image navigation system, the additional light navigation system is designed to achieve the final docking guidance by providing the light for the image navigation system. The detailed principle of light navigation system is in the following.

The light navigation system is composed of a light (green) installed on the docking station, a four-quadrant photoelectric detector installed on the head of UUV as a signal detector. Firstly, a cone-shaped diverging light field is generated, after the four-quadrant photoelectric detector senses the light, the relative position between the UUV and the docking station can be identified through the signal processing. More specifically, as shown in Fig. 10, in order to improve the sensitivity of the four-quadrant photoelectric detector, a convex lens is installed ahead. When the light is condensed by the convex lens, a facula will be formed on the four-quadrant photoelectric detector, whose position can be changed with regard to the posture of the UUV, which can result in the change of current in different quadrants. Finally, the relative position between the UUV and the docking station (green light) can be calculated by the different measured current data.

Therefore, based on the light navigation system in the final docking guidance to generate a green light, the image navigation system can detect the light by the CCD camera when approaching the medium and short distance (less than 50 m), and produce the image-based relative angles (β_s and θ_s), to help increase the accuracy of using only the USBL navigation system. Subsequently, the UUV can accurately approach the docking station, when less than 30 m and the light is bright enough, the four-quadrant photoelectric detector on the UUV works, which can be used to obtain the more accurate relative position when compared to the CCD camera. Finally, the underwater docking task of the UUV is accomplished.

3.5. The data monitoring unit design

The data monitoring unit is mainly used to monitor the state of UUV during the docking process. As shown in Fig. 11, the current longitude, latitude, velocity, roll, pitch and heading angles of UUV are presented

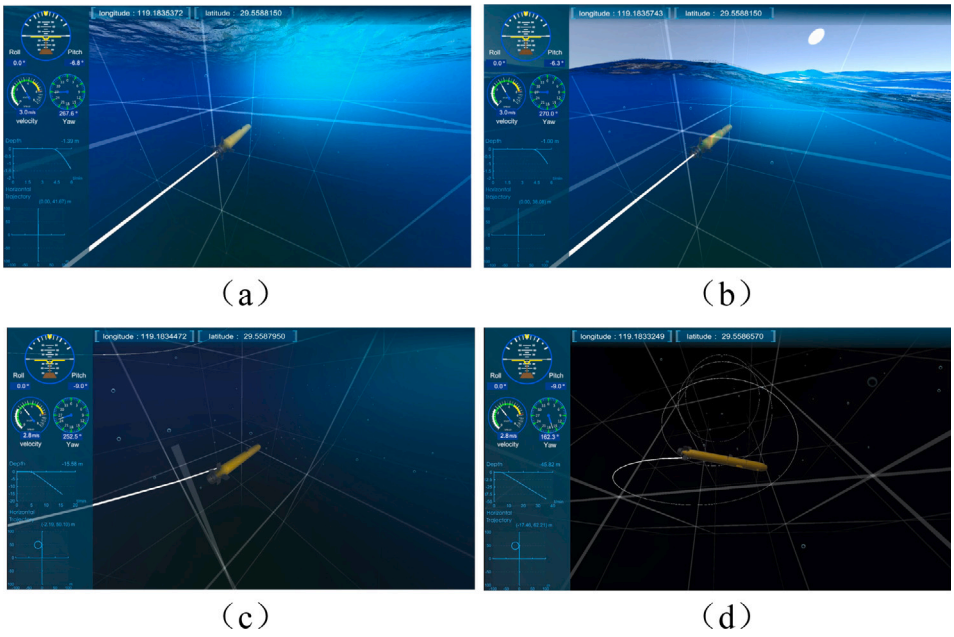

Fig. 12. The process of motion verification. (a) rectilinear motion; (b) downward motion; (c) spiral motion; (d) motion trajectory.

on the interface, which make it clear for operator to observe the process of docking process.

4. Application demonstration for underwater tasks of UUV

Considering the complexity, and expensive cost of underwater tests, it is usually difficult to implement the real experiment to verify the reliability of UUV to achieve underwater docking tasks. Therefore, based on the proposed online simulator with virtual simulation system, the simulation experiment with the motion verification and the underwater docking of UUV are carried out, where the communication between the host and lower computers are achieved by the TCP/IP communication.

4.1. The motion verification of UUV

In order to verify the effectiveness of the motion and control unit design, the motion verification experiment is carried out in the virtual simulation system. The random underwater current is set with the velocity range of $0-0.25$ m/s and direction range of 0–360°, the wave and current on the sea level are described as (1)–(3), the initial position and attitude angle of the UUV are set as $(0,0,0)$ m and $(0,270°,0)$, the desired trajectory is a spiral line and can be given as:

$$x_a = 13.5\cos\left(\frac{\pi}{33}t\right) + 48 \tag{44}$$

$$y_a = 13.5\sin\left(\frac{\pi}{33}t\right) + 15 \tag{45}$$

$$z_d = -\frac{13.5}{66}t \tag{46}$$

Fig. 12 shows the process of the motion verification. At first, the UUV moves in a rectilinear line until the velocity is stable. Then, it moves downward in a uniform velocity with the spiral motion. The data monitoring unit presents the current state of the UUV in real time, such as the longitude, latitude and the motion trajectory. It can also be seen that when the UUV moves downward, the color of the underwater environment becomes darker, which means the virtual simulation system can well simulate the real underwater visual effect in the motion process of the UUV, and provide the researchers with the immersive feeling of the underwater environment when implementing the tasks.

Fig. 13 shows the results of the UUV trajectory tracking in Matlab/simulink. It can be concluded that with the fuzzy PID controller,

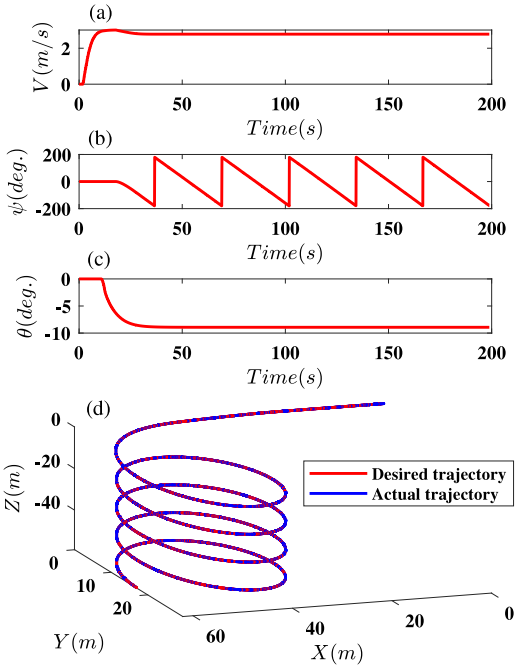

Fig. 13. The results of UUV trajectory tracking in Matlab/simulink. (a) velocity; (b) heading angle; (c) pitch angle; (d) desired and actual motion trajectory.

the motion and control unit can help UUV track the desired trajectory with the certain accuracy under the disturbance of random underwater current. Also, the simulated data can be sent to the virtual simulation system via the TCP/IP communication, which allows the virtual display of the whole process of the motion verification.

4.2. The underwater docking of UUV

In order to verify the effectiveness of the simulated docking process via the whole units proposed in this paper, the underwater docking experiment is carried out in the virtual simulation system, where the

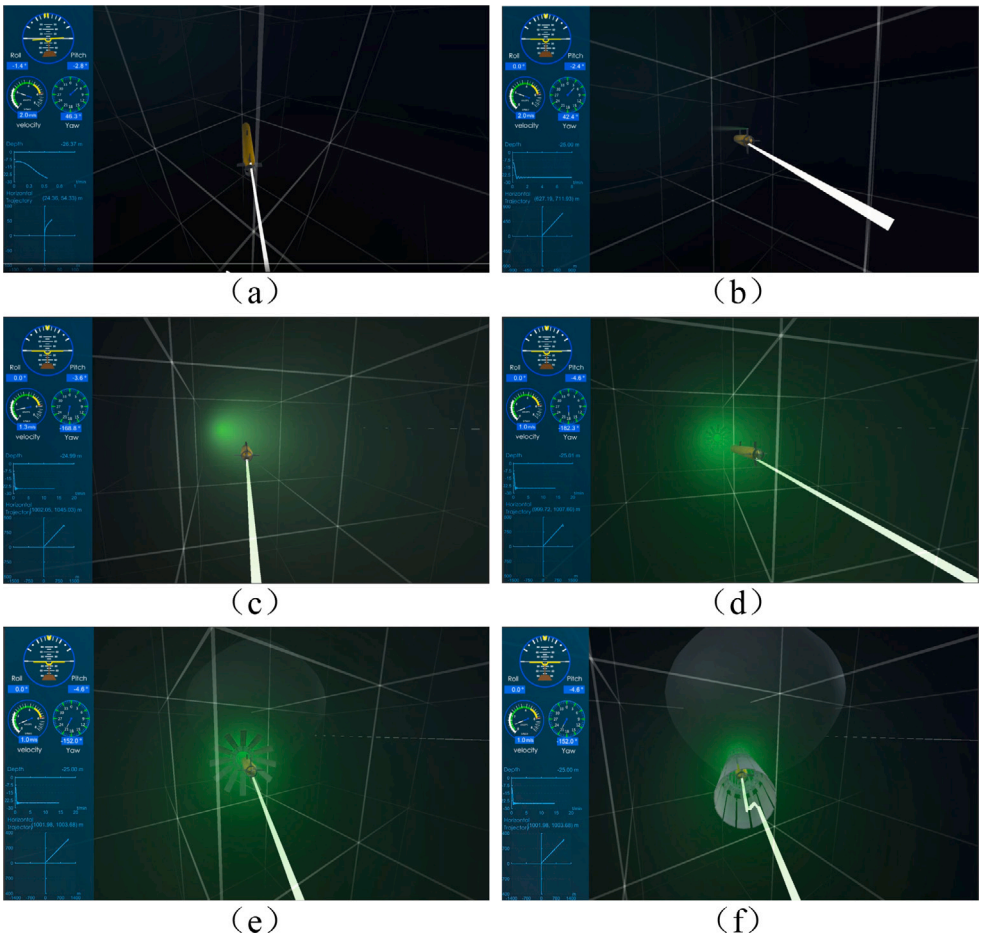

Fig. 14. The process of underwater docking. (a) Period I: remote docking guidance; (b) Period II: medium and long distance docking guidance; (c) Period III: medium and short distance docking guidance; (d) Period IV: final docking guidance; (e) Docking preparation stage; (f) Finish docking.

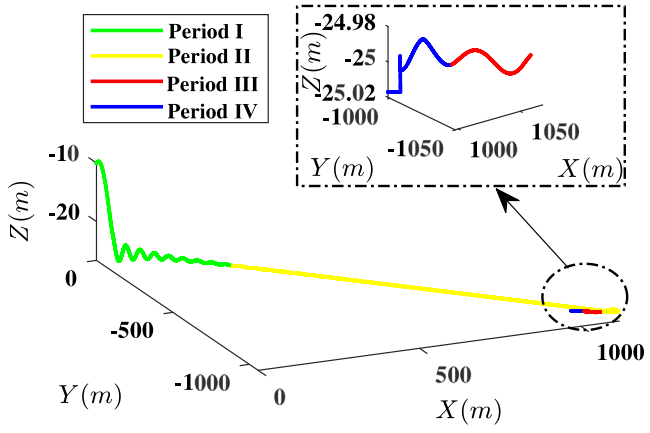

Fig. 15. The trajectory of docking process.

relative position between UUV and docking station is achieved by the docking navigation unit.

Fig. 14 shows the process of underwater docking experiment. Firstly, set the position of docking point, i.e., depth, abscissa and ordinate are set as 25 m, 1000 m, 1000 m, respectively. Besides, set the orientation of the docking station as the same as the initial orientation of the UUV. Since the position of the docking point is larger than 1000 m, which is beyond the range of the acoustic navigation system starting from Period II, the inertial navigation system combined with the doppler speedometer in Period I is set as the first way to implement the docking task, as shown in Fig. 14(a). In details, the inertial navigation system and the doppler speedometer are used to calculate the position and posture of the UUV relative to the docking point, and the data are transmitted to the motion and control unit via the TCP/IP communication, which achieves the motion of UUV towards the docking point, and the data are real-time displayed in the virtual docking scene.

Secondly, when the UUV is within the distance of 1000 m from the docking point, which means it enters the acoustic navigation range, the USBL navigation system in Period II is set as the second way to implement the docking task, as shown in Fig. 14(b), which can obtain the more accurate position and posture of the UUV relative to the docking point.

Subsequently, when the UUV is within the distance of 50 m from docking point, the green light becomes visible, where the image navigation system with a CCD camera in Period III is set as the additional way to help increase the accuracy of the USBL navigation system when implementing the docking task, as shown in Fig. 14(c). By sending the data captured by the CCD camera and the USBL navigation system in Period II, the motion and control unit controls the UUV to adjust its posture to prepare for the final docking.

Finally, when the UUV is within the distance of 30 m from docking point, the green light becomes more bright, where the light navigation system in Period IV is added to help accomplish the docking task, as shown in Fig. 14(d)–(f). In this period, the image and USBL navigation systems are still on. By sending the relative position between the UUV and docking station, which can be calculated by the measured current data obtained from the four-quadrant photoelectric detector,

the motion and control unit can control the UUV to arrive the docking station and finish the docking task. The corresponding trajectory of entire docking process is shown in Fig. 15.

Based on the above analysis, it can be concluded that the online simulator with virtual simulation system can simulate the whole process of the UUV to complete the underwater motion and docking tasks. Moreover, through the underwater tasks simulation of the UUV in the virtual simulation system, it is possible to safely, conveniently, and low-costly provide the researchers with an open interface to simulate the underwater tasks, and also gain experience before the real underwater tests.

5. Conclusion

This paper develops an online simulator with virtual simulation system for the docking tasks of UUV, where the virtual reality technology is used to simulate the real underwater environment and the motion of the UUV. In this virtual simulation system, the lower computer is designed to calculate the mathematical model of the UUV, simulate or interact with the real sensor during the docking process, and transmit the data to the host computer; the host computer is designed to implement the navigation and control of UUV by the use of data obtained from the lower computer. Four different navigation modes and the fuzzy PID controller are designed respectively to implement the tasks in the virtual simulation system, and an open interface is also provided that allows the researchers to test and improve their algorithms before the real underwater test. Two different experiments with the specific motion verification and underwater docking of UUV are implemented, where the processes are immersively and real-time displayed in the virtual docking scene, and the results verify the effectiveness of the online simulator for the underwater tasks simulation with lower cost.

In the future, we will investigate the fault diagnosis methods to fulfill this simulator with more functions, which bring in the dangerous conditions or difficult situations that the UUV may encounter, and help generate or display the corresponding information for the researchers to evaluate the tasks, or allow practice to avoid such conditions or situations in advance.

CRediT authorship contribution statement

Hongjuan Li: Data processing, Validation, Writing – original draft. **Fanghao Huang:** Software, Data processing, Validation, Writing – review & editing. **Zheng Chen:** Conceptualization, Project administration, Writing – review & editing.

Declaration of competing interest

The authors declare that they have no known competing financial interests or personal relationships that could have appeared to influence the work reported in this paper.

Acknowledgments

This work is supported by Key R&D Program of Zhejiang Province (No. 2021C03013), Science Foundation of Donghai Laboratory (No. DH-2022KF01006), and National Natural Science Foundation of China (No. 52075476 and No. 92048302).

Appendix A. Supplementary data

Supplementary material related to this article can be found online at https://doi.org/10.1016/j.oceaneng.2022.112780.

References

Bruno, F., Barbieri, L., Mangeruga, M., Cozza, M., Lagudi, A., et al., 2019. Underwater augmented reality for improving the diving experience in submerged archaeological sites. Ocean Eng. 190, 106487.

Bukhari, A.C., Kim, Y.G., 2013. A research on an intelligent multipurpose fuzzy semantic enhanced 3D virtual reality simulator for complex maritime missions. Appl. Intell. 38 (2), 193–209.

Chen, Z., Huang, F., Chen, W., Zhang, J., Sun, W., Chen, J., Gu, J., Zhu, S., 2020a. RBFNN-based adaptive sliding mode control design for delayed nonlinear multilateral tele-robotic system with cooperative manipulation. IEEE Trans. Ind. Inf. 16 (2), 1236–1247.

Chen, Z., Li, C., Yao, B., Yuan, M., Yang, C., 2020b. Integrated coordinated/synchronized contouring control of A dual-linear-motor-driven gantry. IEEE Trans. Ind. Electron. 67 (5), 3944–3954.

de la Cruz, Marcos, Casan, Gustavo A., Sanz, Pedro J., Marín, Ral, 2020. A new virtual reality interface for underwater intervention missions. IFAC-PapersOnLine 53 (2), 14600–14607.

Faure, C., et al., 2020. Adding haptic feedback to virtual environments with a cable-driven robot improves upper limb spatio-temporal parameters during a manual handling task. IEEE Trans. Neural Syst. Rehabil. Eng. 28 (10), 2246–2254.

Huang, F., Chen, X., Chen, Z., Pan, Y.-J., 2022a. A novel SMMS teleoperation control framework for multiple mobile agents with obstacles avoidance by leader selection. IEEE Transactions on Systems, Man, and Cybernetics: Systems 1–13. http://dx.doi.org/10.1109/TSMC.2022.3199112, (in press).

Huang, F., Yang, X., Chen, Z., Chen, J., Mei, D., 2022b. Design and evaluation of visual-and-force-assisted virtual operation system for underwater teleoperation training. Journal of Intelligent Manufacturing (in press).

Huang, H., Zhang, S., Yang, Z., Tian, Y., Zhao, X., et al., 2018. Modified smith fuzzy PID temperature control in an oil-replenishing device for deep-sea hydraulic system. Ocean Eng. 149, 14–22.

Kluger, D.T., et al., 2019. Virtual reality provides an effective platform for functional evaluations of closed-loop neuromyoelectric control. IEEE Trans. Neural Syst. Rehabil. Eng. 27 (5), 876–886.

Lipton, J.I., Fay, A.J., Rus, D., 2018. Baxter's homunculus: Virtual reality spaces for teleoperation in manufacturing. IEEE Robot. Autom. Lett. 3 (1), 179–186.

Makavita, C.D., Jayasinghe, S.G., Nguyen, H.D., Ranmuthugala, D., 2019. Experimental study of a command Governor adaptive depth controller for an unmanned underwater vehicle. Appl. Ocean Res. 86, 61–72.

Melo, J., Matos, A., 2017. Survey on advances on terrain based navigation for autonomous underwater vehicles. Ocean Eng. 139, 250–264.

Miao, J., Wang, S., Zhao, Z., Li, Y., Tomovic, M.M., 2017. Spatial curvilinear path following control of underactuated AUV with multiple uncertainties. ISA Trans. 67, 107–130.

Monferrer, A., Bonyuet, D., 2002. Cooperative robot teleoperation through virtual reality interfaces. In: Proceedings Sixth International Conference on Information Visualisation. pp. 243–248.

Mu, X., He, B., Wu, S., Zhang, X., Song, Y., Yan, T., 2021. A practical INS/GPS/DVL/PS integrated navigation algorithm and its application on autonomous underwater vehicle. Appl. Ocean Res. 106, 102441.

Nie, Y., Luan, X., Gan, W., Ou, T., Song, D., 2020. Design of marine virtual simulation experiment platform based on Unity3D. In: Global Oceans 2020. Singapore-U.S. Gulf Coast, pp. 1–5.

Peral-Boiza, M., et al., 2019. Position based model of a flexible ureterorenoscope in a virtual reality training platform for a minimally invasive surgical robot. IEEE Access 7, 177414–177426.

Qi, X., Xiang, P., Cai, Z., 2020. Spatial target path following and coordinated control of multiple UUVs. Int. J. Nav. Archit. Ocean Eng. 12, 832–842.

Sahoo, A., Dwivedy, S.K., Robi, P.S., 2019. Advancements in the field of autonomous underwater vehicle. Ocean Eng. 181, 145–160.

Sarhadi, P., Noei, A.R., Khosravi, A., 2016. Adaptive integral feedback controller for Pitch and Yaw channels of an AUV with actuator saturations. ISA Trans. 65, 284–295.

Sun, W., Tang, S., Gao, H., Zhao, J., 2016. Two time-scale tracking control of nonholonomic wheeled mobile robots. IEEE Trans. Control Syst. Technol. 24 (6), 2059–2069.

Wang, J., Chen, X., Yang, P., 2021a. Adaptive H-infinite Kalman filter based on multiple fading factors and its application in unmanned underwater vehicle. ISA Trans. 108, 295–304.

Wang, Q., Jiao, W., Yu, R., Johnson, M.T., Zhang, Y., 2020. Virtual reality robot-assisted welding based on human intention recognition. IEEE Trans. Autom. Sci. Eng. 17 (2), 799–808.

Wang, F., Wan, L., Su, Ym., et al., 2010. AUV modeling and motion control strategy design. J. Mar. Sci. Appl. 9, 379–385.

Wang, T., Zhao, Q., Yang, C., 2021b. Visual navigation and docking for a planar type AUV docking and charging system. Ocean Eng. 224, 108744.

Yuan, M., Chen, Z., Yao, B., Hu, J., 2019. A general online trajectory planning framework in the case of desired function unknown in advance. IEEE Trans. Ind. Inf. 15 (5), 2753–2762.

Zhang, W., Teng, Y., Wei, S., Xiong, H., Ren, H., 2018. The robust H-infinity control of UUV with Riccati equation solution interpolation. Ocean Eng. 156, 252–262.